

# The hidden risks of temporal resampling in clinical reinforcement learning

Thomas Frost<sup>1\*</sup>, Hrisheekesh Vaidya<sup>1</sup>, and Steve Harris<sup>1,2</sup>

<sup>1</sup>University College London, London, United Kingdom

<sup>2</sup>University College London Hospitals NHS Foundation Trust, London, United Kingdom

\*Corresponding author: thomas.frost.21@ucl.ac.uk

## Abstract

Offline reinforcement learning (ORL) has shown potential for improving decision-making in healthcare. However, contemporary research typically aggregates patient data into fixed time intervals, simplifying their mapping to standard ORL frameworks. The impact of these temporal manipulations on model safety and efficacy remains poorly understood. In this work, using both a gridworld navigation task and the UVA/Padova clinical diabetes simulator, we demonstrate that temporal resampling significantly degrades the performance of offline reinforcement learning algorithms during live deployment. We propose three mechanisms that drive this failure: (i) the generation of counterfactual trajectories, (ii) the distortion of temporal expectations, and (iii) the compounding of generalisation errors. Crucially, we find that standard off-policy evaluation metrics can fail to detect these drops in performance. Our findings reveal a fundamental risk in current healthcare ORL pipelines and emphasise the need for methods that explicitly handle the irregular timing of clinical decision-making.

## INTRODUCTION

Reinforcement learning (RL) is a machine-learning approach where an agent learns, through repeated interactions with an environment, a set of decision-making policies that maximise long-term rewards. While this framework has achieved superhuman performance in robotics<sup>1</sup> and gameplay<sup>2</sup>, its clinical application is limited by the safety risks of direct experimentation on patients<sup>3</sup>. To address this, healthcare-based research has primarily focused on offline reinforcement learning<sup>4</sup> (ORL), in which agents attempt to infer optimal policies using retrospective clinical datasets. Recent applications include optimising fluid and vasopressor dosing in sepsis<sup>5–7</sup>, personalising chemotherapy<sup>8,9</sup>, improving ventilation management in intensive care<sup>10,11</sup>, and automating insulin delivery in diabetes<sup>12</sup>.

To assess whether these RL models are safe for deployment on real patients, they are typically assessed using off-policy evaluation (OPE) on retrospective data. Techniques such as importance sampling<sup>13,14</sup> and fitted Q-evaluation<sup>15,16</sup> (FQE) aim to predict a policy’s real-world performance, screening out unsafe or ineffective models. However, the reliability of OPE – and ORL generally – depends on

how well the dataset represents the full range of patient states and clinical decisions the model might encounter. If a policy steers patient physiology into unfamiliar territory, a failure to generalise to these out-of-distribution states can lead to unpredictable or dangerous recommendations. This phenomenon, known as *distributional shift*<sup>17</sup>, is challenging for OPE to estimate because evaluation accuracy is fundamentally limited by the support of the known data. Despite being a well-recognised problem in ORL<sup>4</sup>, the risks of distributional shift remain underappreciated in healthcare due to a scarcity of prospective studies<sup>18</sup> and a general over-reliance on OPE.

A potential source for distributional shift is temporal resampling during data preprocessing. In healthcare machine learning, electronic health record (EHR) data are commonly aggregated – or, less frequently, interpolated – into fixed time intervals to address irregular clinical sampling<sup>19,20</sup>. Within clinical ORL, this serves a dual purpose: it provides structure to high-dimensional features and ensures decision labels occur at steady intervals. The latter is particularly convenient for the Markov decision process (MDP) framework commonly used in ORL, which assumes actions occur in discrete, regular steps<sup>21–23</sup>. Consequently, temporal resampling has become a near-universal workaround in clinical ORL; the majority of recent studies resample observations, actions, and rewards into evenly spaced windows, typically 4-hour aggregates<sup>5,10–12,24–40</sup>.

However, clinical decision-making is inherently sporadic and event-driven: clinicians may intervene immediately in a crisis or wait hours during periods of stability. While alternative frameworks exist to account for variable decision intervals – most notably the semi-Markov decision process (SMDP)<sup>41–43</sup> – their use within clinical ORL remains rare<sup>44</sup>. Despite the widespread reliance on resampling and MDPs, their use could result in distributional shift by fundamentally altering the model’s perception of the environmental dynamics. To our knowledge, the impact of this practice on model performance at deployment has never been formally evaluated, likely due to the lack of safe, readily accessible testing environments in healthcare.

In this study, we utilise two simulated environments to generate datasets of offline reinforcement learning and examine the impact of temporal resampling on prospective model performance. Specifically, we test two primary hypotheses. First, we believe temporal resampling of decisions may promote harmful distributional shift by training models on data that misrepresent the underlying environment’s dynamics. Second, this shift may be poorly detectable by off-policy evaluation (OPE) because such methods are conducted on post-processed data, without access to the true underlying data distribution.

We validate these hypotheses using two reinforcement learning environments modified for irregular time intervals: the LavaGap 2D navigation task<sup>45</sup> and the FDA-approved UVA/Padova simulator for insulin management of type 1 diabetes<sup>46</sup>. LavaGap is selected for its simplicity to clearly demonstrate any effects of temporal resampling. In contrast, the UVA/Padova simulator provides a clinically realistic setting with continuous insulin infusions, mirroring high-stakes decisions like the titration of vasopressors commonly studied in healthcare ORL. We conclude with methodological recommendations to address these issues in future research.

## RESULTS

## Dataset generation

We conducted experiments in two simulated environments: LavaGap, a partially observable gridworld requiring navigation around hazards (Figure 1), and UVA/Padova, an FDA-approved clinical simulator for type 1 diabetes mellitus (T1DM). Both environments were implemented in two configurations: a regular version with fixed time steps and an irregular version where variable intervals mimic the sporadic nature of clinical interventions. From each irregular environment, we used an expert agent to generate an unprocessed dataset that preserves the true variable intervals between decisions. The unprocessed dataset was then cloned and preprocessed into two variants: (1) a binned dataset, which downsamples observations and rewards via aggregation into broad, fixed time windows; and (2) an interpolated dataset, which upsamples the decision frequency such that a de Full specifications and data generation details are

## Temporal binning leads to counterfactual training data

An example of a simulated patient trajectory in UVA/Padova, before and after temporal binning, is shown in Figure 2. The top panel displays real-time changes in blood glucose and insulin sampled at the environment's 10-minute base frequency, with variable-length plateaus in the insulin infusion rate reflecting the irregular decision intervals. The bottom panel shows the effect of a typical 2-hour binning regimen. For blood glucose, broader trends are preserved, with binning acting as a low-pass filter with only modest information loss. Conversely, insulin actions deviate significantly: brief, high-frequency spikes are dampened and replaced by gradual changes. As a result, a model trained on binned data will misattribute the observed glucose dynamics to these artificially gradual changes in insulin delivery.

Temporal binning can also reverse the causal ordering of events in training data. This is demonstrated in the bottom panel of Figure 2 (red circle). In the unprocessed trajectory, the final observed carbohydrate load is followed by a sharp increase in insulin delivery, which counteracts the subsequent rise in blood glucose. However, after temporal binning, the averaging windows align such that the insulin increase appears to occur before the carbohydrate intake, reversing the order of these events. This artifact arises because observations are averaged over the window immediately preceding the action (see Methods). While averaging over the same window could resolve this specific inconsistency, it would introduce look-ahead bias; the observation would already be confounded by the future effects of the action the model is trying to learn<sup>47</sup>. This specific type of confounding is explored further by Tang et al. in their recent work on this problem.

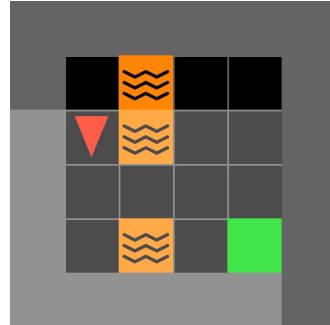


Figure 1: LavaGap Environment: To reach the green goal square, the agent (red triangle) must navigate the grid without contacting the lava (orange squares). The model uses partial observations (light grey) to calculate the optimal path. The episode ends with a reward of 1 if the agent reaches the goal, or 0 if it hit lava or exceeded the maximum number of steps.

upsamples the decision frequency such that a decision is recorded at every environmental time step. Full specifications and data generation details are provided in the Methods.

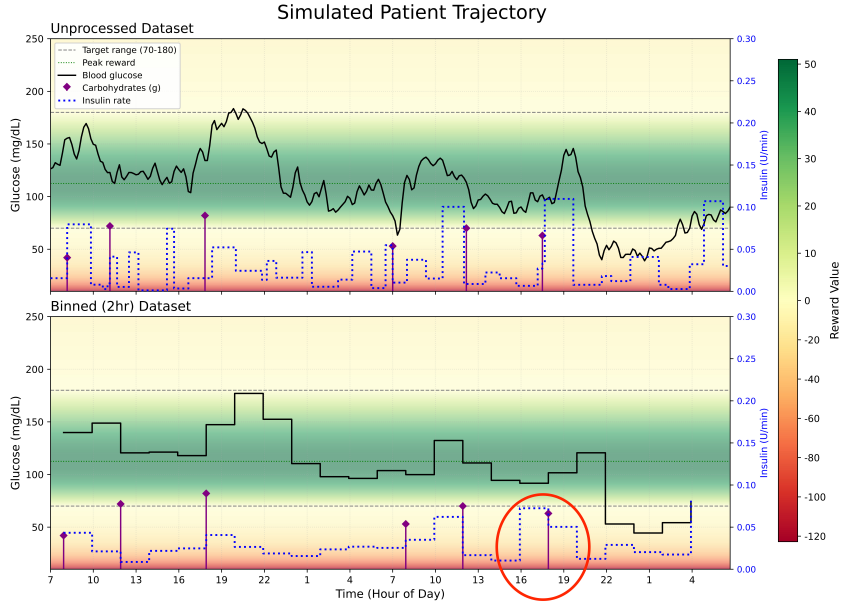


Figure 2: Example patient trajectory in the UVA/Padova simulator, before (top panel) and after (bottom panel) temporal binning. Background shading indicates the reward landscape, with positive (green) rewards in the target glycaemic range and negative (red) rewards for hypo- or hyperglycaemia. An example of a counterfactual trajectory that reverses cause and effect is shown circled in the lower panel.

### Resampling degrades the performance of offline reinforcement learning models

We assessed the impact of temporal resampling (both binning and interpolation) on several offline reinforcement learning algorithms: behavioural cloning (BC), implicit Q-learning (IQL), and conservative Q-learning (CQL). IQL and CQL are widely regarded as state-of-the-art model-free methods for offline RL, demonstrating robust performance across diverse discrete and continuous control tasks. In contrast, BC serves as a supervised learning baseline by attempting to directly mimic the dataset's behaviour rather than optimise for long-term rewards. For each algorithm, identical neural networks were trained on the three dataset variants and evaluated in both the regular and irregular versions of each environment. We used an MDP formulation for the binned and interpolated datasets and an SMDP formulation for the unprocessed dataset.

The results for the LavaGap environment are shown in Figure 3a, compared against the proximal policy optimisation (PPO) expert baseline. Only agents trained on the unprocessed dataset were able to improve upon the baseline; the interpolated and binned datasets resulted in performance consistently below the expert level. This deterioration persisted across both the irregular and regular versions of the environment. Training on the temporally binned dataset consistently resulted in the poorest performance, likely because binning removes the greatest amount of temporally relevant information – both through data aggregation and the loss of variable decision intervals. By contrast, the interpolated dataset avoids aggregation and differs from the unprocessed dataset only in that it treats each time step as an independent decision. We explore the implications of this finding further in the Discussion.

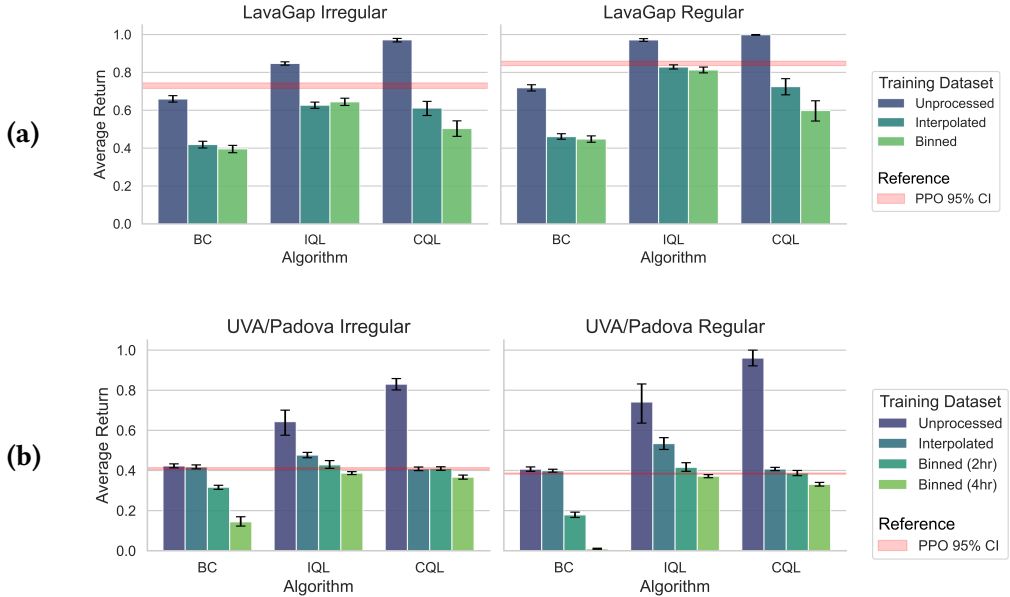


Figure 3: Impact of temporal resampling on offline RL performance. Agents trained via behavioural cloning (BC), implicit Q-learning (IQL), or conservative Q-learning (CQL) were evaluated on (a) the discrete LavaGap navigation task and (b) the continuous UVA/Padova insulin control task. Models were trained using unprocessed, interpolated, or temporally binned datasets and deployed in both regular and irregular versions of the environment. In both domains, agents trained on the unprocessed dataset consistently achieved the highest returns, whereas binned and interpolated datasets led to significant performance degradation. The pink band indicates the expert proximal policy optimisation (PPO) baseline used to generate the training data. For UVA/Padova, average returns are normalised (0.0 for a random policy; 1.0 for the highest observed score). Shaded regions and error bars represent 95% confidence intervals (CIs).

Replicating these experiments in the more complex UVA/Padova environment yielded broadly similar patterns (Figure 3b). The unprocessed dataset consistently produced the highest average returns for both CQL and IQL, substantially outperforming the PPO baseline. Performance declined monotonically as the level of temporal abstraction increased: interpolation led to better results than 2-hour binning, which in turn outperformed 4-hour binning. Unlike in LavaGap, IQL models trained on the interpolated dataset in UVA/Padova occasionally exceeded the baseline, though these gains remained modest and fell well short of the performance achieved with the unprocessed dataset.

### **Off-policy evaluation can be overoptimistic on binned data**

Next, we examined how the accuracy of off-policy evaluation using fitted Q-evaluation<sup>15</sup> (FQE) varies with the choice of training dataset in the UVA/Padova environment. For each algorithm-dataset pair, we trained an FQE model to predict the agent’s expected return and compared these estimates against the agent’s true performance in the irregular environment. Figure 4 presents these results as a calibration plot relative to each dataset’s baseline performance. Overall, FQE models trained on the unprocessed and interpolated datasets showed reasonably high calibration, accurately estimating the returns of the IQL and CQL agents. In contrast, FQE severely overestimated the performance of agents trained on binned data, predicting 1.5–3x improvements for agents that, in reality, only matched or underperformed their respective baselines.

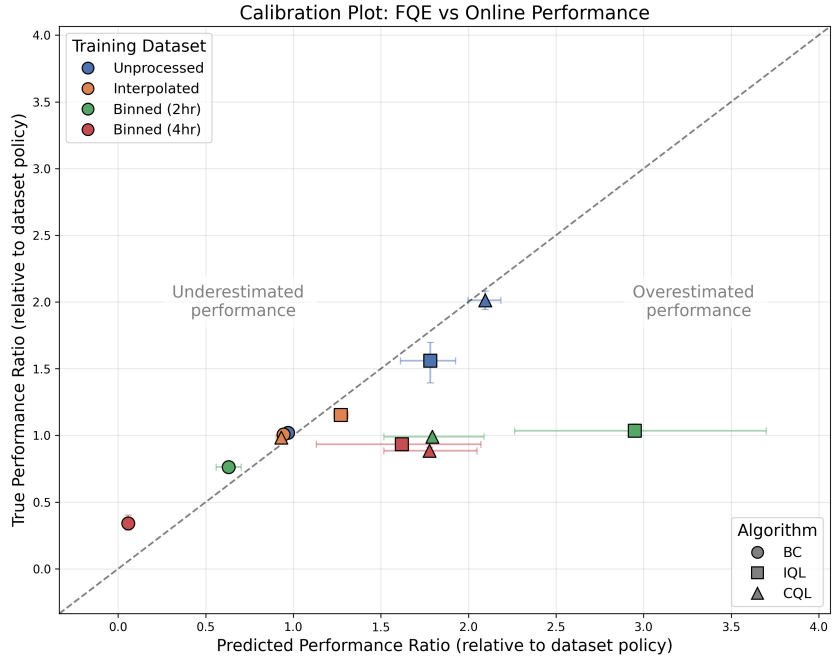


Figure 4: Calibration plot showing reliability of off-policy evaluation across different types of dataset preprocessing. The plot compares the true online performance of trained agents in the UVA/Padova environment against the performance predicted by fitted Q-evaluation (FQE). Performance is normalised such that 0.0 represents a random policy and 1.0 represents the dataset’s behaviour policy. While agents trained on unprocessed (blue) and interpolated (orange) data show high calibration (clustering near the diagonal), those trained on temporally binned data (green, red) exhibit severe overestimation bias. Error bars represent 95% confidence intervals.

This systematic overestimation likely reflects the fact that IQL and CQL are solving for actions that appear highly favourable within the binned datasets, even if such actions are suboptimal in reality. When FQE is conducted on the same post-processed data, its predictions become similarly optimistic. However, because the binned dataset contains trajectories that are counterfactual – unlike the unprocessed or interpolated datasets – these predictions amount to hallucinations rather than accurate estimates. This finding highlights a central concern raised in our introduction: that the widespread use of OPE on temporally binned data may substantially overestimate the clinical utility of the resulting reinforcement learning models.

## DISCUSSION

In this work, we demonstrate that temporal resampling, a common preprocessing step in offline reinforcement learning for healthcare, can lead to substantial performance degradation when these models are deployed in real time. Using two simulated environments with irregular decision intervals, we show that agents trained on temporally discretised data fail to generalise well when reintroduced to the original irregular environment. Moreover, this failure may be poorly detected by off-policy evaluation, the current standard in assessing healthcare ORL. We attribute this failure to OPE being conducted on post-processed data rather than ground-truth trajectories. We will now propose several mechanisms to explain these phenomena.

First, temporal binning generates counterfactual patient trajectories by aggregating states, actions, and rewards into broad intervals. This smoothing process creates fictitious data that obscures clinically meaningful dynamics. For example, a 4-hour bin (commonly seen in sepsis-based ORL research) might average severe blood pressure fluctuations into a deceptively stable mean. Similarly, aggregating high-frequency interventions can produce ‘artificial decisions’ that never took place and therefore did not drive the observed outcomes. As demonstrated in Figure 2, window positioning can even reverse the causal sequence of events. Because these counterfactual trajectories do not correspond to real clinical events, they compromise the generalisability of the learned policy to the true underlying environment.

Second, decision resampling distorts the agent’s expectation of temporal dynamics. For example, by training on interpolated datasets with uniformly short intervals, the agent learns to anticipate frequent opportunities to revise its actions (e.g., every 10 minutes). Consequently, the policy is optimised under the false assumption that decisions can be adjusted often. At deployment, if the actual interval between decisions is significantly longer, this mismatch can induce harmful behaviour, such as over- or under-dosing medication because the anticipated decision opportunity never arrived. This discrepancy likely explains why agents trained on interpolated data consistently underperformed in irregular environments, despite the training data appearing superficially similar to the unprocessed ground truth.

Third, training an agent on high-frequency interpolated data and deploying it into an environment with regular intervals appears to increase sensitivity to distributional shift. This is likely explained by the compounding of generalisation errors at deployment; as the agent makes more frequent decisions, small errors accumulate, driving the system into ‘out-of-distribution’ regions of the state space. If a single sustained action (e.g., a 2-hour infusion) is reframed as a series of independent high-frequency actions (e.g., 120 one-minute decisions), the cumulative opportunity for error increases proportionally. Our results suggest that this heightened risk far outweighs any theoretical benefit from having more intervention opportunities. Notably, this occurs even under the ‘ideal’ conditions of our interpolated dataset, which utilises ground-truth intermediate observations rather than imputed values. Consequently, we advise caution when training agents on irregular or low-frequency data for deployment into high-frequency settings.

As an alternative solution to temporal resampling and its associated risks, we propose retaining naturally irregular intervals between decision labels and utilising reinforcement learning frameworks that explicitly account for them (such as the SMDP framework employed in this work). As demonstrated by our results, this approach provides the model with the most accurate representation of the environment’s temporal dynamics, resulting in the greatest capacity to improve upon the dataset’s baseline behaviour. It is important, however, to distinguish between irregularly sampled decision labels and irregularly sampled input data. While our experiments focus on the former, many healthcare datasets also suffer from the latter, where observations are recorded sporadically (often characterised as ‘missingness’). While a comprehensive review of techniques for handling irregularly sampled observations is beyond the scope of this work, we direct the reader to several recent architectures designed to process such inputs without relying on temporal resampling<sup>48–51</sup>.

This study has several limitations. First, our clinical results were conducted within a continuous action space; we have not yet demonstrated that these findings extend to discrete action spaces in a clinical setting. Similarly, we used a direct method estimator (fitted Q-evaluation) for off-policy evaluation, as importance sampling-based estimators are problematic in continuous domains. Since both discrete action spaces and importance sampling are prevalent in existing healthcare ORL literature, this may restrict the immediate generalisability of our OPE findings. Furthermore, our analysis was restricted to model-free algorithms and does not include model-based methods, which are less common in this field. Finally, our simulated environments feature relatively low-dimensional observation spaces, which may be more sensitive to the information loss induced by binning; high-dimensional real-world datasets,

characterised by a wider range of physiological features, may be more robust to these effects.

In summary, our findings demonstrate that forcing sporadic clinical decisions into a discretised MDP framework through temporal resampling can lead to a fundamental misalignment between the offline reinforcement learning model and the true dynamics of the environment. This may introduce model weaknesses that are not only detrimental to performance but are also unlikely to be detected by standard off-policy evaluation. Our results suggest that transitioning to mathematical frameworks that naturally account for irregular decision-making, such as the SMDP framework used here and in other works<sup>44</sup>, may fully address these issues. We therefore recommend that future research in healthcare ORL moves beyond default binning practices, prioritising RL frameworks that preserve the temporal patterns inherent in clinical decision-making.

## METHODS

### Preliminaries

Reinforcement learning conventionally uses a Markov decision process (MDP) to model the interaction between the agent and the environment. We define an MDP by the tuple  $\mathcal{M} = (\mathcal{S}, \mathcal{A}, T, \mu_0, r, \gamma)$ , where:

- $s_t \in \mathcal{S}$  is the state at time  $t$  (e.g., the physiological state of the patient) within the state space  $\mathcal{S}$ ;
- $a_t \in \mathcal{A}$  is the action taken at time  $t$  from the available action space  $\mathcal{A}$ ;
- $\mu_0$  is a probability distribution over  $\mathcal{S}$ , with the initial state  $s_0 \sim \mu_0$ ;
- $T(s_{t+1}|s_t, a_t) : \mathcal{S} \times \mathcal{A} \rightarrow \Delta(\mathcal{S})$  is the transition kernel, representing the probability of reaching state  $s_{t+1}$  given the current  $s_t$  and  $a_t$ ;
- $R : \mathcal{S} \times \mathcal{A} \times \mathcal{S} \rightarrow \mathbb{R}$  is the reward function, where  $r_{t+1} = R(s_t, a_t, s_{t+1})$ ;
- $\gamma \in [0, 1]$  is the discount factor, determining the present value of future rewards.

If the observations from the environment are only a partial reflection of the true underlying state (such as in healthcare), this is treated as a partially observable MDP (POMDP), with additional elements:

- $o_t \in \mathcal{O}$ , the observations perceived at time  $t$  (e.g., blood pressure, heart rate) from the observation space  $\mathcal{O}$ ;
- $Z(o_t|s_t, a_{t-1}) : \mathcal{S} \times \mathcal{A} \rightarrow \Delta(\mathcal{O})$ , the observation model representing the probability of perceiving  $o_t$  given the current true state  $s_t$  and previous action  $a_{t-1}$ .

The policy  $\pi$  of the agent generates actions  $a_t$  in response to states  $s_t$  (or observations  $o_t$ ), aiming to maximise the expected cumulative discounted return:

$$J(\pi) = \mathbb{E}_{\tau \sim (\pi, T, \mu_0)} \left[ \sum_{t=0}^{\infty} \gamma^t R(s_t, a_t, s_{t+1}) \right] \quad (1)$$

where the trajectory  $\tau = (s_0, a_0, s_1, a_1, \dots)$  represents some sequence of environmental interactions.

If the time intervals between agent decisions are variable, the environment can be considered as a semi-Markov decision process (SMDP). In this setting, we distinguish between time steps  $t$  (the underlying clock time) and decision epochs  $k$ . If the  $k$ -th decision occurs at time  $t_k$ , the system remains in a state  $s_k$  for some finite duration  $\Delta t_k = t_{k+1} - t_k$  after taking action  $a_k$ , before transitioning to the next state  $s_{k+1}$  at the next decision epoch. The transition dynamics are defined by a joint distribution over the next state and the duration:

$$T(s_{k+1}, \Delta t | s_k, a_k)$$

The reward accumulated during this interval,  $r_{k+1}$ , is the discounted sum of atomic rewards  $p$  collected at each underlying time step between  $t_k$  and  $t_{k+1}$ :

$$r_{k+1} = R(s_k, a_k, s_{k+1}, \Delta t) = \mathbb{E} \left[ \sum_{i=0}^{\Delta t-1} \gamma^i p_{t_k+i+1} \mid s_k, a_k, s_{k+1}, \Delta t \right] \quad (2)$$

The agent's objective in this setting is to maximise the expected return discounted by the cumulative real-time duration. Letting  $t_k$  denote the actual time at the  $k$ -th decision epoch (where  $t_k = \sum_{i=0}^{k-1} \Delta t_i$ ), the objective is:

$$J(\pi) = \mathbb{E}_{\tau \sim (\pi, T, \mu_0)} \left[ \sum_{k=0}^{\infty} \gamma^{t_k} R(s_k, a_k, s_{k+1}, \Delta t_k) \right] \quad (3)$$

To avoid ambiguity, within this manuscript we use *time steps* to denote the smallest unit of environmental transition; *actions* to denote the inputs applied to the environment at each time step; and *decisions* to denote the agent's chosen action, which may be repeated across multiple time steps in an SMDP.

### **Simulated environments**

We conducted our experiments in two simulated environments, modified to support irregular decision intervals.

#### **LavaGap**

LavaGap<sup>45</sup> is a partially observable, two-dimensional gridworld in which the agent must reach a green goal square while avoiding orange lava pits (Figure 1). The agent views the observable pixels and selects one of several discrete actions: move forward, rotate left or right, or do nothing. Each episode returns a reward of 1 if the agent reaches the goal, and 0 if it falls into lava or exceeds the 100-step limit.

#### **UVA/Padova**

The UVA/Padova simulator<sup>46</sup> is an FDA-approved clinical diabetes simulator comprising 300 virtual patients with type 1 diabetes mellitus (T1DM). It is accepted as a substitute for pre-clinical animal research studies, including closed-loop "artificial pancreas" algorithm studies, prior to human clinical trials. For our experiments, we used a customised implementation including 30 patients (10 adults, 10 adolescents, 10 children)<sup>52</sup>. Each patient has a number of individualised physiological parameters, such as glycogen stores, insulin sensitivity, and gastric emptying rate. The observation space consists of current blood glucose, the insulin infusion rate, time of day, and any carbohydrate intake since the previous observation. The continuous action space represents the current basal insulin infusion rate. Each environmental time step lasts 10 minutes. Episodes terminate after 48 hours, or earlier if glucose levels become dangerously low (< 10 mg/dL) or high (> 600 mg/dL).

The 30 patients were partitioned into three distinct cohorts: a training cohort of 18 patients (used for all training experiments), and validation and testing cohorts of 6 patients each. All cohorts maintained an equal split of adult, adolescent, and child patients.

The reward function is derived from the Magni risk index<sup>53</sup> (Equation 4), which is a function of the patient's blood glucose level. We shift this by a constant to set positive rewards in the euglycaemic range (70–180 mg/dL), and apply a max operator to increase the magnitude of positive rewards relative to negative rewards (Equation 5). The reward landscape is visualised in Supplementary Figure S1. The environment additionally returns a -10,000 penalty for terminating early due to extreme blood glucose levels.

$$g(x) = 10 \cdot (1.509 \cdot (\ln(x)^{1.084} - 5.381))^2 \quad (4)$$

$$R(x) = \max(5.1 - g(x), 10 \cdot (5.1 - g(x))) \quad (5)$$

### Regular and Irregular Variants

In both environments, we implemented a regular version, in which each agent decision covers exactly one time step, and an irregular version, in which decisions are applied after a variable number of elapsed time steps. In LavaGap Irregular, intervals between decisions alternate stochastically between 1 and 3 time steps. In UVA/Padova Irregular, intervals are sampled from a uniform distribution over 1 to 12 time steps.

### Dataset generation

To generate datasets for offline learning, we first trained a proximal policy optimisation (PPO) agent<sup>54</sup> to solve the irregular version of each environment, with regular model checkpoints during training. In UVA/Padova, the agent was trained on the training cohort of patients, with each checkpoint evaluated over a fixed number of episodes using the validation cohort of patients. We selected an intermediate checkpoint achieving approximately 70–80% of the agent’s best overall performance to serve as the ‘expert policy’. This ensures the dataset demonstrates competent but imperfect behaviour, providing room for offline agents to improve.

Using this expert policy, we generated a ground-truth reference dataset by interacting repeatedly with the environment’s irregular version (100,000 transitions for LavaGap; 10 million for UVA/Padova). From this reference dataset, we constructed three dataset versions:

1. **Unprocessed dataset:** Records all state transitions and a mask identifying independent agent decisions, preserving the semi-MDP structure.
2. **Interpolated dataset:** Identical to the unprocessed dataset, but treats all transitions as independent decisions. For example, in UVA/Padova, a decision held for 60 minutes is treated as six independent 10-minute decisions.
3. **Binned dataset:** Produced via temporal binning. In LavaGap, every second time step was subsampled. In UVA/Padova, windows (2- or 4-hours) were used to average observations/actions and sum rewards. Observations were aggregated over the preceding window to avoid look-ahead bias.

All UVA/Padova datasets had their rewards standardised to zero mean and unit variance using values from the training datasets. No other preprocessing was performed, as the environments already internally normalise their observations.

### Offline training

#### Algorithms

We evaluated the effect of each dataset using three algorithms: behavioural cloning<sup>55</sup> (BC), implicit Q-learning<sup>56</sup> (IQL), and conservative Q-learning<sup>57</sup> (CQL). BC serves as a supervised learning baseline. IQL and CQL are state-of-the-art model-free methods that constrain the learned policy to stay within the support of the training data.

For the binned and interpolated datasets, standard MDP formulations were used.

For the unprocessed dataset, we adapted IQL and CQL to the semi-MDP setting by calculating the discounted sum of rewards over the holding period  $\Delta t$  and modifying the Bellman backup. For example, the IQL critic loss becomes:

$$L_Q(\theta) = \frac{1}{2} \mathbb{E}_{(s,a,r,s',\Delta t) \sim \mathcal{D}} [(r + \gamma^{\Delta t} V_\psi(s') - Q_\theta(s, a))^2] \quad (6)$$

where  $r$  is the cumulative discounted reward accrued during  $\Delta t$  as defined in Equation 2.

### Model Architecture

For each environment, all experiments used the same model architecture consisting of a feature encoder and one or more decoding heads, with Leaky ReLU activation for hidden layers.

- **LavaGap:** A convolutional neural network (CNN) feature encoder followed by dense multi-layer perceptron (MLP) decoding heads.
- **UVA/Padova:** An MLP followed by a long short-term memory (LSTM) layer for the feature encoder, and MLPs for each decoding head.

In the discrete-action LavaGap environment, all policy and critic networks produced output vectors with dimensionality matching the action space. In the continuous-action UVA/Padova environment, the policy network output the  $\alpha$  and  $\beta$  parameters of a Beta distribution<sup>58</sup>, scaled to the insulin infusion range (0–0.5 U/min). Critic networks incorporated the action by concatenating it with the latent state representation. During dataset generation, actions were sampled from the PPO action distribution. All evaluation tasks used deterministic outputs corresponding to the action with the highest probability for LavaGap and the distributional mean for UVA/Padova.

### Evaluation

Agarwal et al.<sup>59</sup> describe a statistically robust protocol for analysing reinforcement learning experiments, which we follow here. Each experiment (defined by a specific ORL algorithm-dataset pair) consisted of 50 independent training runs with different random seeds.

- **Training:** Offline agents for LavaGap were trained for 10,000 update steps. Agents for UVA/Padova were trained for up to 100,000 update steps, with early stopping based on performance on the validation cohort.
- **Evaluation:** Upon completion of training, the offline agent was deployed in both the regular and irregular versions of the environment (using the test cohort for UVA/Padova). Performance was evaluated over 100 episodes in LavaGap and 30 episodes per test patient in UVA/Padova, with results averaged to obtain a mean score for each run.
- **Statistical Analysis:** Scores from the 50 runs were aggregated using the interquartile mean (IQM) to improve robustness to outlier performances. We computed 95% confidence intervals using stratified bootstrapping with 100,000 replicates.

In addition, for UVA/Padova, we performed off-policy evaluation using fitted Q-evaluation (FQE)<sup>15</sup>. For each run, an FQE model was trained for 30,000 update steps to estimate the value of the learned policy using the same static dataset employed for policy training. An equivalent dataset of 3 million transitions was generated using the test patient cohort, and inference was performed on the initial states of this dataset to produce an FQE score for that run. The same statistical analysis as in the online evaluation was applied, including aggregation via the IQM and stratified bootstrapping. The original PPO agent used to generate the dataset was used as a baseline, both explicitly (by evaluating PPO in the live environment) and implicitly (by conducting FQE on the offline dataset behaviour).

## Computing details

Models were implemented in Python (v3.10) using PyTorch<sup>60</sup> (v2.9.0). Custom environments used Gymnasium<sup>61</sup> (0.29.1) and our own Numba-accelerated version of SimGlucose<sup>52</sup> (0.2.11). We used the Adam optimiser for all training<sup>62</sup>, with default PyTorch hyperparameters aside from learning rate.

Critics in IQL and CQL used clipped double Q-networks. Target networks were updated using Polyak averaging with  $\alpha = 0.005$ . A full table of hyperparameters is provided in Table 1. For the IQL and CQL hyperparameters, a preliminary hyperparameter sweep was performed to identify stable optima consistent across all three temporal resampling regimes, ensuring comparisons were not biased by dataset-specific tuning. A REFORMS checklist<sup>63</sup> is provided in Supplementary Table S1.

Table 1: Hyperparameters for LavaGap and UVA/Padova environments.

Hyperparameters	LavaGap	UVA/Padova	UVA/Padova (FQE)
Learning rate	$1 \cdot 10^{-3}$	$3 \cdot 10^{-4}$	$3 \cdot 10^{-4}$
Batch size	64	1024	256
Hidden dimensions	64	128	64
$\gamma$ - discount factor	0.99	0.99	1.0
$\tau$ - expectile (IQL)	0.8	0.9	–
$\beta$ - temperature (IQL)	10	10	–
$\alpha$ - reg. term (CQL)	1.0	1.0	–
$\alpha$ - entropy term (CQL)	0.2	0.0	–

## DATA AND CODE AVAILABILITY

The datasets generated and analysed during this study are available from the corresponding author upon reasonable request. The authors intend to release the code used for environment simulation, data generation, and model training publicly in the near future following publication.

## AUTHOR CONTRIBUTION

All authors have read and approved this manuscript. TF and HV designed the experiments. TF wrote the software code, which HV checked. TF analysed the experimental results. TF and HV wrote the manuscript. SH provided supervision.

## ACKNOWLEDGEMENTS

This study was funded by EPSRC as part of the UKRI Centre for Doctoral Training in AI for Healthcare (grant EP/S021612/1). The funder played no role in study design, data collection, analysis and interpretation of data, or the writing of this manuscript. The views expressed in the text are those of the authors and not necessarily those of the funders. We also acknowledge the facilities provided by University College London, which helped enabled this research. Finally, we thank Ahmed Al-Hindawi, Jennifer Hunter, Aasiyah Rashan, Dan Stein, Dylan Whitaker, and Matt Wilson for their valued input during the preparation of this manuscript.

## ETHICS DECLARATIONS

All authors declare no competing interests. No ethical approval was required for this research.

## REFERENCES

- [1] Tang, C. *et al.* Deep reinforcement learning for robotics: A survey of real-world successes. *Annual Review of Control, Robotics, and Autonomous Systems* **8** (2024).
- [2] Shakya, A. K., Pillai, G. & Chakrabarty, S. Reinforcement learning algorithms: A brief survey. *Expert Systems with Applications* **231**, 120495 (2023).
- [3] Jayaraman, P., Desman, J., Sabourchi, M., Nadkarni, G. N. & Sakhija, A. A primer on reinforcement learning in medicine for clinicians. *NPJ Digital Medicine* **7**, 337 (2024).
- [4] Levine, S., Kumar, A., Tucker, G. & Fu, J. Offline reinforcement learning: Tutorial, review, and perspectives on open problems. *arXiv preprint arXiv:2005.01643* (2020).
- [5] Komorowski, M., Celi, L. A., Badawi, O., Gordon, A. C. & Faisal, A. A. The artificial intelligence clinician learns optimal treatment strategies for sepsis in intensive care. *Nature medicine* **24**, 1716–1720 (2018).
- [6] Liu, R. *et al.* Offline reinforcement learning with uncertainty for treatment strategies in sepsis. *arXiv preprint arXiv:2107.04491* (2021).
- [7] Fatemi, M., Killian, T. W., Subramanian, J. & Ghassemi, M. Medical dead-ends and learning to identify high-risk states and treatments. *Advances in Neural Information Processing Systems* **34**, 4856–4870 (2021).
- [8] Liu, Y. *et al.* Deep reinforcement learning for dynamic treatment regimes on medical registry data. In *2017 IEEE international conference on healthcare informatics (ICHI)*, 380–385 (IEEE, 2017).
- [9] Shiranthika, C. *et al.* Supervised optimal chemotherapy regimen based on offline reinforcement learning. *IEEE Journal of Biomedical and Health Informatics* **26**, 4763–4772 (2022).
- [10] Prasad, N., Cheng, L.-F., Chivers, C., Draugelis, M. & Engelhardt, B. E. A reinforcement learning approach to weaning of mechanical ventilation in intensive care units. *arXiv preprint arXiv:1704.06300* (2017).
- [11] Kondrup, F. *et al.* Towards safe mechanical ventilation treatment using deep offline reinforcement learning. In *Proceedings of the Thirty-Seventh AAAI Conference on Artificial Intelligence and Thirty-Fifth Conference on Innovative Applications of Artificial Intelligence and Thirteenth Symposium on Educational Advances in Artificial Intelligence, AAAI'23/IAAI'23/EAAI'23* (AAAI Press, 2023). URL <https://doi.org/10.1609/aaai.v37i13.26862>.
- [12] Wang, G. *et al.* Optimized glycemic control of type 2 diabetes with reinforcement learning: a proof-of-concept trial. *Nature medicine* **29**, 2633–2642 (2023). URL <http://dx.doi.org/10.1038/s41591-023-02552-9>.

- [13] Precup, D., Sutton, R. S. & Singh, S. P. Eligibility traces for off-policy policy evaluation. In *Proceedings of the Seventeenth International Conference on Machine Learning*, ICML '00, 759–766 (Morgan Kaufmann Publishers Inc., San Francisco, CA, USA, 2000).
- [14] Thomas, P. S., Theocharous, G. & Ghavamzadeh, M. High confidence off-policy evaluation. In *Proceedings of the Twenty-Ninth AAAI Conference on Artificial Intelligence*, AAAI'15, 3000–3006 (AAAI Press, 2015).
- [15] Le, H., Voloshin, C. & Yue, Y. Batch policy learning under constraints. In *International Conference on Machine Learning*, 3703–3712 (PMLR, 2019).
- [16] Hao, B. *et al.* Bootstrapping fitted q-evaluation for off-policy inference. In *International Conference on Machine Learning*, 4074–4084 (PMLR, 2021).
- [17] Kumar, A., Fu, J., Soh, M., Tucker, G. & Levine, S. Stabilizing off-policy q-learning via bootstrapping error reduction. *Advances in neural information processing systems* **32** (2019).
- [18] Otten, M. *et al.* Does reinforcement learning improve outcomes for critically ill patients? A systematic review and level-of-readiness assessment. *Critical care medicine* **52**, e79–e88 (2024). URL <http://dx.doi.org/10.1097/CCM.0000000000006100>.
- [19] Lipton, Z. C., Kale, D. C., Wetzel, R. *et al.* Modeling missing data in clinical time series with rnns. *Machine Learning for Healthcare* **56**, 253–270 (2016).
- [20] Shukla, S. N. & Marlin, B. M. A survey on principles, models and methods for learning from irregularly sampled time series. *arXiv preprint arXiv:2012.00168* (2020).
- [21] Bellman, R. A markovian decision process. *Journal of mathematics and mechanics* 679–684 (1957).
- [22] Puterman, M. L. *Markov decision processes: discrete stochastic dynamic programming* (John Wiley & Sons, 2014).
- [23] Sutton, R. S. & Barto, A. G. *Reinforcement learning: An introduction* (MIT press, 2018).
- [24] Nemati, S., Ghassemi, M. M. & Clifford, G. D. Optimal medication dosing from suboptimal clinical examples: a deep reinforcement learning approach. *Annual International Conference of the IEEE Engineering in Medicine and Biology Society. IEEE Engineering in Medicine and Biology Society. Annual International Conference* **2016**, 2978–2981 (2016). URL <https://pubmed.ncbi.nlm.nih.gov/28268938/>.
- [25] Yu, C., Liu, J. & Zhao, H. Inverse reinforcement learning for intelligent mechanical ventilation and sedative dosing in intensive care units. *BMC medical informatics and decision making* **19**, 57 (2019). URL <http://dx.doi.org/10.1186/s12911-019-0763-6>.
- [26] Kim, Y., Suescun, J., Schiess, M. C. & Jiang, X. Computational medication regimen for Parkinson's disease using reinforcement learning. *Scientific reports* **11**, 9313 (2021). URL <http://dx.doi.org/10.1038/s41598-021-88619-4>.
- [27] Peine, A. *et al.* Development and validation of a reinforcement learning algorithm to dynamically optimize mechanical ventilation in critical care. *npj digital medicine* **4**, 32 (2021). URL <http://dx.doi.org/10.1038/s41746-021-00388-6>.

- [28] Sun, C., Hong, S., Song, M., Shang, J. & Li, H. Personalized vital signs control based on continuous action-space reinforcement learning with supervised experience. *Biomedical signal processing and control* **69**, 102847 (2021). URL <http://dx.doi.org/10.1016/j.bspc.2021.102847>.
- [29] Eghbali, N., Alhanai, T. & Ghassemi, M. M. Patient-specific sedation management via deep reinforcement learning. *Frontiers in digital health* **3**, 608893 (2021). URL <http://dx.doi.org/10.3389/fdgth.2021.608893>.
- [30] Roggeveen, L. *et al.* Transatlantic transferability of a new reinforcement learning model for optimizing haemodynamic treatment for critically ill patients with sepsis. *Artificial intelligence in medicine* **112**, 102003 (2021). URL <http://dx.doi.org/10.1016/j.artmed.2020.102003>.
- [31] Yala, A. *et al.* Optimizing risk-based breast cancer screening policies with reinforcement learning. *Nature medicine* **28**, 136–143 (2022). URL <http://dx.doi.org/10.1038/s41591-021-01599-w>.
- [32] Guo, H., Li, J., Liu, H. & He, J. Learning dynamic treatment strategies for coronary heart diseases by artificial intelligence: real-world data-driven study. *BMC medical informatics and decision making* **22**, 39 (2022). URL <http://dx.doi.org/10.1186/s12911-022-01774-0>.
- [33] Nanayakkara, T., Clermont, G., Langmead, C. J. & Swigon, D. Unifying cardiovascular modelling with deep reinforcement learning for uncertainty aware control of sepsis treatment. *PLOS digital health* **1**, e0000012 (2022). URL <http://dx.doi.org/10.1371/journal.pdig.0000012>.
- [34] Li, T., Wang, Z., Lu, W., Zhang, Q. & Li, D. Electronic health records based reinforcement learning for treatment optimizing. *Information systems* **104**, 101878 (2022). URL <http://dx.doi.org/10.1016/j.is.2021.101878>.
- [35] Su, L. *et al.* Establishment and implementation of potential fluid therapy balance strategies for ICU sepsis patients based on reinforcement learning. *Frontiers in medicine* **9**, 766447 (2022). URL <http://dx.doi.org/10.3389/fmed.2022.766447>.
- [36] Liang, D., Deng, H. & Liu, Y. The treatment of sepsis: an episodic memory-assisted deep reinforcement learning approach. *Applied intelligence* **53**, 11034–11044 (2023). URL <http://dx.doi.org/10.1007/s10489-022-04099-7>.
- [37] Wu, X., Li, R., He, Z., Yu, T. & Cheng, C. A value-based deep reinforcement learning model with human expertise in optimal treatment of sepsis. *npj digital medicine* **6**, 15 (2023). URL <http://dx.doi.org/10.1038/s41746-023-00755-5>.
- [38] den Hengst, F. *et al.* Guideline-informed reinforcement learning for mechanical ventilation in critical care. *Artificial intelligence in medicine* **147**, 102742 (2024). URL <http://dx.doi.org/10.1016/j.artmed.2023.102742>.
- [39] Kalimouttou, A. *et al.* Optimal vasopressin initiation in septic shock: The OVISS reinforcement learning study. *JAMA: the journal of the American Medical Association* (2025). URL <https://jamanetwork.com/journals/jama/fullarticle/2831858>.
- [40] Desman, J. M. *et al.* A distributional reinforcement learning model for optimal glucose control after cardiac surgery. *npj Digital Medicine* **8**, 313 (2025).

- [41] Jewell, W. S. Markov-renewal programming. i: Formulation, finite return models. *Operations Research* **11**, 938–948 (1963).
- [42] Bradtke, S. & Duff, M. Reinforcement learning methods for continuous-time markov decision problems. *Advances in neural information processing systems* **7** (1994).
- [43] Sutton, R. S., Precup, D. & Singh, S. Between mdps and semi-mdps: A framework for temporal abstraction in reinforcement learning. *Artificial intelligence* **112**, 181–211 (1999).
- [44] Fatemi, M. *et al.* Semi-markov offline reinforcement learning for healthcare. In *Conference on Health, Inference, and Learning*, 119–137 (PMLR, 2022).
- [45] Chevalier-Boisvert, M. *et al.* Minigrid & miniworld: Modular & customizable reinforcement learning environments for goal-oriented tasks. In *Advances in Neural Information Processing Systems 36, New Orleans, LA, USA* (2023).
- [46] Man, C. D. *et al.* The uva/padova type 1 diabetes simulator: new features. *Journal of diabetes science and technology* **8**, 26–34 (2014).
- [47] Tang, S., Yao, J., Wiens, J. & Parbhoo, S. Off by a beat: Temporal misalignment in offline rl for healthcare. In *RLC 2025 Workshop on Practical Insights into Reinforcement Learning for Real Systems* (2025).
- [48] Che, Z., Purushotham, S., Cho, K., Sontag, D. & Liu, Y. Recurrent neural networks for multivariate time series with missing values. *Scientific reports* **8**, 6085 (2018).
- [49] Kidger, P., Morrill, J., Foster, J. & Lyons, T. Neural controlled differential equations for irregular time series. *Advances in neural information processing systems* **33**, 6696–6707 (2020).
- [50] Shukla, S. N. & Marlin, B. M. Multi-time attention networks for irregularly sampled time series. *arXiv preprint arXiv:2101.10318* (2021).
- [51] Tipirneni, S. & Reddy, C. K. Self-supervised transformer for sparse and irregularly sampled multivariate clinical time-series. *ACM Transactions on Knowledge Discovery from Data (TKDD)* **16**, 1–17 (2022).
- [52] Xie, J. Simglucose v0.2.1. <https://github.com/jxx123/simglucose> (2018). Accessed: Oct-04-2025.
- [53] Kovatchev, B. P., Cox, D. J., Gonder-Frederick, L. A. & Clarke, W. Symmetrization of the blood glucose measurement scale and its applications. *Diabetes care* **20**, 1655–1658 (1997).
- [54] Schulman, J., Wolski, F., Dhariwal, P., Radford, A. & Klimov, O. Proximal policy optimization algorithms. *arXiv preprint arXiv:1707.06347* (2017).
- [55] Kumar, A., Hong, J., Singh, A. & Levine, S. When should we prefer offline reinforcement learning over behavioral cloning? *arXiv preprint arXiv:2204.05618* (2022).
- [56] Kostrikov, I., Nair, A. & Levine, S. Offline reinforcement learning with implicit q-learning. *arXiv preprint arXiv:2110.06169* (2021).
- [57] Kumar, A., Zhou, A., Tucker, G. & Levine, S. Conservative q-learning for offline reinforcement learning. *Advances in neural information processing systems* **33**, 1179–1191 (2020).

- [58] Chou, P.-W., Maturana, D. & Scherer, S. Improving stochastic policy gradients in continuous control with deep reinforcement learning using the beta distribution. In *International conference on machine learning*, 834–843 (PMLR, 2017).
- [59] Agarwal, R., Schwarzer, M., Castro, P. S., Courville, A. C. & Bellemare, M. Deep reinforcement learning at the edge of the statistical precipice. *Advances in neural information processing systems* **34**, 29304–29320 (2021).
- [60] Paszke, A. *et al.* Pytorch: An imperative style, high-performance deep learning library. *Advances in neural information processing systems* **32** (2019).
- [61] Towers, M. *et al.* Gymnasium: A standard interface for reinforcement learning environments. *arXiv preprint arXiv:2407.17032* (2024).
- [62] Kingma, D. P. Adam: A method for stochastic optimization. *arXiv preprint arXiv:1412.6980* (2014).
- [63] Kapoor, S. *et al.* Reforms: Consensus-based recommendations for machine-learning-based science. *Science Advances* **10**, eadk3452 (2024).

## **Supplementary Figure 1**

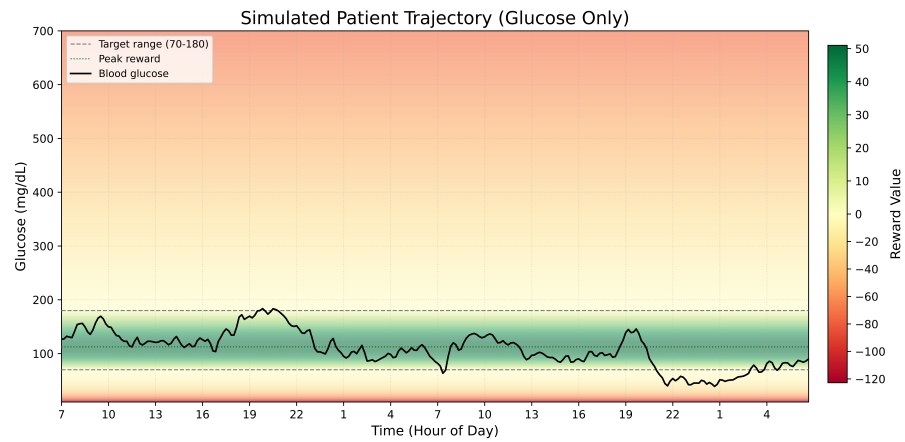


Figure S1: Extension of Figure 2, showing the full reward landscape for all permissible glucose levels in the UVA/Padova T1DM simulator.

## Supplementary Table 1

REFORMS checklist, as per Kapoor et al.<sup>63</sup>

Item	Description	Page	Notes
<b>Module 1: Study goals</b>			
1a	Population or distribution about which the scientific claim is made.	9	Simulated environments: LavaGap (gridworld) and UVA/Padova T1DM simulator (30 virtual patients: adults, adolescents, children).
1b	Motivation for choosing this population or distribution (1a.).	2	LavaGap for "simplicity to clearly demonstrate effects," UVA/Padova for "clinically realistic setting... high-stakes decisions".
1c	Motivation for the use of ML methods in the study.	2	Clinical application of RL is limited by safety; Offline RL (ORL) allows inference from retrospective data without patient risk.
<b>Module 2: Computational reproducibility</b>			
2a	Dataset used for training and evaluating the model along with link or DOI to uniquely identify the dataset.	10	Datasets were generated uniquely by interacting with the LavaGap and UVA/Padova environments (see Methods).
2b	Code used to train and evaluate the model and produce the results reported in the paper along with link or DOI to uniquely identify the version of the code used.	12	Code available on reasonable request, with plans for public release.
2c	Description of the computing infrastructure used.	12	Python (v3.10), PyTorch (v2.9.0), Gymnasium (0.29.1), Numba-accelerated SimGlucose. (See Methods).
2d	README file which contains instructions for generating the results using the provided dataset and code.	12	Code available on reasonable request, with plans for public release.
2e	Reproduction script to produce all results reported in the paper.	12	Code available on reasonable request, with plans for public release.
<b>Module 3: Data quality</b>			
3a	Source(s) of data, separately for the training and evaluation datasets (if applicable), along with the time when the dataset(s) are collected, the source and process of ground-truth annotations, and other data documentation.	10	Expert PPO policy used to generate 100k transitions (LavaGap) and 10M transitions (UVA/Padova). (See Methods - Dataset generation).
3b	Distribution or set from which the dataset is sampled (i.e., the sampling frame).	10	Transitions generated from interacting with the "irregular version" of each environment.
3c	Justification for why the dataset is useful for the modeling task at hand.	2	Allows for offline RL algorithms trained on the dataset to be evaluated live in the corresponding simulated environment.
3d	The definition of the outcome variable of the model along with descriptive statistics, if applicable.	11	The interquartile mean with 95% confidence intervals, following the procedure described in the Methods.
3e	Number of samples in the dataset.	10	100,000 transitions (LavaGap); 10,000,000 transitions (UVA/Padova).

Item	Description	Page	Notes
3f	Percentage of missing data, split by class for a categorical outcome variable.	10	0% missing data (generated from simulated environments).
3g	Justification for why the distribution or set from which the dataset is drawn (3b.) is representative of the one about which the scientific claim is being made (1a.).	2	The datasets are generated directly from the target simulators (LavaGap/UVA-Padova), ensuring models trained on these data should (theoretically) perform well when evaluated in the matching environment.
<b>Module 4: Data preprocessing</b>			
4a	Identification of whether any samples are excluded with a rationale for why they are excluded.	9	UVA/Padova: 12 patients excluded from training - 6 for validation, 6 for testing.
4b	How impossible or corrupt samples are dealt with.	9	N/A for LavaGap. For UVA/Padova, episodes terminated early if glucose < 10 mg/dL or > 600 mg/dL (with a -10,000 penalty).
4c	All transformations of the dataset from its raw form (3a.) to the form used in the model, for instance, treatment of missing data and normalization.	10	Temporal binning (2h/4h), interpolation, and reward standardization to zero mean/unit variance (see Methods).
<b>Module 5: Modeling</b>			
5a	Detailed descriptions of all models trained, including:	10	BC, IQL, and CQL algorithms trained using identical neural networks across three dataset variants (unprocessed, binned, interpolated).
	All features used in the model (including any feature selection).	9	LavaGap: partial grid pixels. UVA/Padova: blood glucose, insulin rate, time of day, and carbohydrate intake.
	Types of models implemented (e.g., Random Forests, Neural Networks).	11	LavaGap: CNN encoder with MLP heads. UVA/Padova: MLP + LSTM encoder (to handle temporal dependencies) with MLP heads.
	Loss function used.	10	Standard MSE for BC; IQL/CQL critic loss $L_Q(\theta)$ modified with SMDP Bellman backups for variable intervals $\Delta t$ .
5b	Justification for the choice of model types implemented.	10	IQL/CQL selected as state-of-the-art model-free offline RL; BC used as a supervised learning baseline.
5c	Method for evaluating the model(s) reported in the paper, including details of train-test splits or cross-validation folds.	11	50 independent runs per experiment. UVA/Padova uses a 6-patient test cohort (30 episodes/patient); LavaGap uses 100 episodes.
5d	Method for selecting the model(s) reported in the paper.	11	UVA/Padova: early stopping based on validation cohort performance. LavaGap: trained for fixed 10,000 update steps.
5e	For the model(s) reported in the paper, specify details about the hyperparameter tuning:		

Item	Description	Page	Notes
	Range of hyper-parameters used and a justification for why this range is reasonable.	12	Parameters were explored via a preliminary search to identify regions of stable optima across all three temporal resampling regimes.
	Method to select the best hyper-parameter configuration.	12	The final configuration was selected by confirming consistent stable performance across all dataset variants, ensuring comparisons were not biased by dataset-specific tuning.
	Specification of all hyper-parameters used to generate results reported in the paper.	12	Described in Table 1
5f	Justification that model comparisons are against appropriate baselines.	11	Compared against the PPO expert baseline (representative of the baseline that generated the original training dataset).
<b>Module 6: Data leakage</b>			
6a	Justification that pre-processing (Section 4) and modeling (Section 5) steps only use information from the training dataset (and not the test dataset).	11	All training data and normalization parameters were calculated strictly using the training patient cohort (18-patient cohort for UVA/Padova).
6b	Methods to address dependencies or duplicates between the training and test datasets (e.g. different samples from the same patients are kept in the same dataset partition).	9	Data leakage was prevented by partitioning the 30 virtual patients in UVA/Padova into mutually exclusive training (18), validation (6), and test (6) cohorts.
6c	Justification that each feature or input used in the model is legitimate for the task at hand and does not lead to leakage.	9	For UVA/Padova, all observations (blood glucose, carbohydrate, insulin, time of day) are from the past/present only, with no leakage of future information. Any aggregation of observations was done using the preceding window only (to avoid look-ahead bias). LavaGap uses the immediately observable pixels only.
<b>Module 7: Metrics and uncertainty</b>			
7a	All metrics used to assess and compare model performance (e.g., accuracy, AUROC etc.). Justify that the metric used to select the final model is suitable for the task.	11	Primary metric: cumulative undiscounted return (interquartile mean), representing the true live performance of the model in the environment. FQE used for off-policy estimation of the same metric.
7b	Uncertainty estimates (e.g., confidence intervals, standard deviations), and details of how these are calculated.	11	95% confidence intervals calculated using the procedure described in the Methods.
7c	Justification for the choice of statistical tests (if used) and a check for the assumptions of the statistical test.	11	No formal p-value-based hypothesis tests were used; comparison is based on non-overlapping 95% CIs as per Agarwal et al. (2021).
<b>Module 8: Generalizability and limitations</b>			
8a	Evidence of external validity.		Not reported. External validation was not performed as the study was conducted within simulated environments (LavaGap and UVA/Padova).

Item	Description	Page	Notes
8b	Contexts in which the authors do not expect the study's findings to hold.	7	Results may vary in discrete clinical action spaces or high-dimensional real-world data where physiological features may be more robust to binning.